TMT Labeling for the Masses: A Robust and Cost-efficient, In-solution Labeling Approach

Authors

Jana Zecha, Shankha Satpathy, Tamara Kanashova, Shayan C. Avanessian, M. Harry Kane, Karl R. Clauser, Philipp Mertins, Steven A. Carr, and Bernhard Kuster

Correspondence

kuster@tum.de;
scarr@broad.mit.edu

In Brief

Isobaric labeling using tandem mass tags (TMTs) is increasingly applied for deep-scale proteomic studies in a multitude of organisms and addressing diverse research questions. The cost of labeling reagents represents a substantial proportion of the total expenses for conducting such experiments. Here, Zecha *et al.* present an economically optimized TMT labeling approach that reduces the quantity of required labeling reagent by a factor of eight and reproducibly achieves complete labeling.

Graphical Abstract

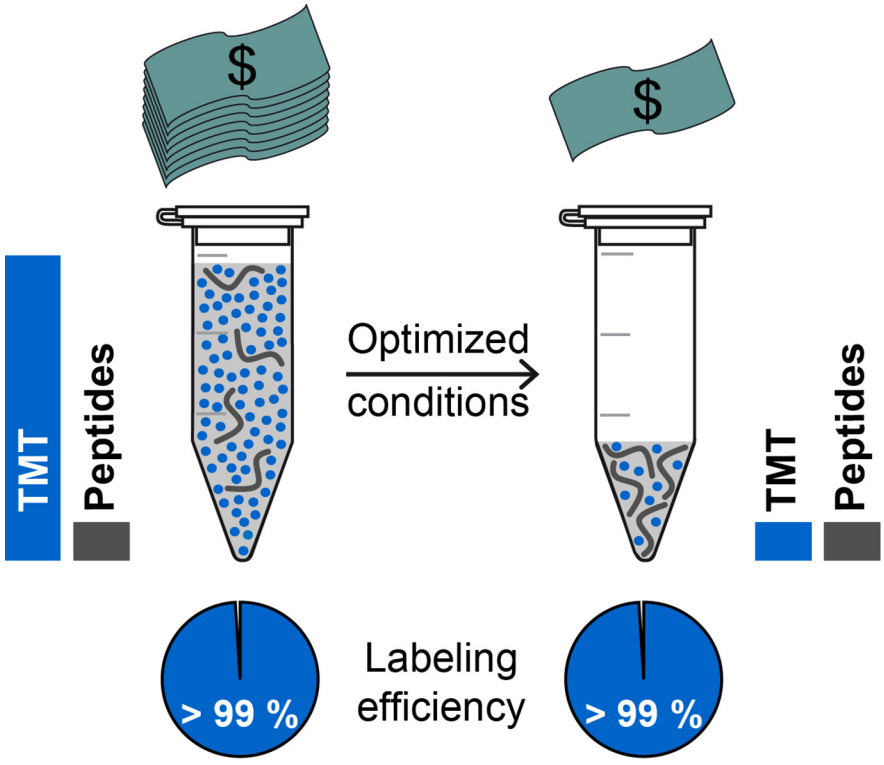

Highlights

- TMT labeling protocol with excellent intra- and interlaboratory reproducibility.
- Complete in-solution labeling of peptides using 1/8 of recommended TMT quantities.
- Demonstration of utility for deep-scale (phospho)proteome analysis.

Zecha et al., 2019, Molecular & Cellular Proteomics *18*, 1468–1478

https://doi.org/10.1074/mcp.TIR119.001385

TMT Labeling for the Masses: A Robust and Cost-efficient, In-solution Labeling Approach*[S]

Jana Zecha‡, Shankha Satpathy§, Tamara Kanashova¶, Shayan C. Avanessian§, M. Harry Kane§, Karl R. Clauser§, Philipp Mertins§¶‖, Steven A. Carr§‡‡, and Bernhard Kuster‡**§§

Isobaric stable isotope labeling using, for example, tandem mass tags (TMTs) is increasingly being applied for large-scale proteomic studies. Experiments focusing on proteoform analysis in drug time course or perturbation studies or in large patient cohorts greatly benefit from the reproducible quantification of single peptides across samples. However, such studies often require labeling of hundreds of micrograms of peptides such that the cost for labeling reagents represents a major contribution to the overall cost of an experiment. Here, we describe and evaluate a robust and cost-effective protocol for TMT labeling that reduces the quantity of required labeling reagent by a factor of eight and achieves complete labeling. Under- and overlabeling of peptides derived from complex digests of tissues and cell lines were systematically evaluated using peptide quantities of between 12.5 and 800 μg and TMT-to-peptide ratios (wt/wt) ranging from 8:1 to 1:2 at different TMT and peptide concentrations. When reaction volumes were reduced to maintain TMT and peptide concentrations of at least 10 mM and 2 g/l, respectively, TMT-to-peptide ratios as low as 1:1 (wt/wt) resulted in labeling efficiencies of > 99% and excellent intra- and interlaboratory reproducibility. The utility of the optimized protocol was further demonstrated in a deep-scale proteome and phosphoproteome analysis of patient-derived xenograft tumor tissue benchmarked against the labeling procedure recommended by the TMT vendor. Finally, we discuss the impact of labeling reaction parameters for N-hydroxysuccinimide ester-based chemistry and provide guidance on adopting efficient labeling protocols for different peptide quantities. ***Molecular & Cellular Proteomics 18: 1468–1478, 2019. DOI: 10.1074/mcp.TIR119.001385.***

In bottom-up proteomics, a variety of strategies can be followed to determine quantitative differences in the abundance of proteins and posttranslational modifications (PTMs) (1). Among those, stable isotope labeling of peptides using isobaric reagents such as tandem mass tags (TMTs) enables multiplexing of up to 11 samples (2). Each of these 11 tags can be used to label primary amines in peptide digests via the reaction with the NHS ester-based reactive group. Subsequently, all samples are pooled and further processed together, thus reducing technical variation in the experimental workflow. Inside the mass spectrometer, the isobaric nature of the tags leads to a summation of each peptide signal from all labeled and combined samples in the MS1 spectrum. Following peptide fragmentation, sample-specific reporter ions of different mass-to-charge (*m/z*) values are generated from the different tags owing to the different combinations of heavy carbon and nitrogen isotopes present in the reporter ions. This enables the differentiation and relative quantification of peptides from all conditions in the same MS2 scan. Multiplexing in this manner greatly reduces the number of missing peptide quantification values in each TMT experiment. Further, quantification reproducibility is less sensitive to performance variations of the liquid chromatography (LC)[1] and mass spectrometry (MS) systems than for label-free measurements. In addition, the multiplexing capability of TMT reagents enables achieving deep proteome coverage for multiple samples in a reasonable amount of measurement time. Together these advantages render isobaric tags attractive for MS-based proteoform studies, including posttranslational modifications analyses that depend on robust quantification of single peptides across conditions (3). The high intra- and interlaboratory reproducibility of a TMT workflow for deep-scale proteome and phosphoproteome analyses has recently been demonstrated for patient-derived xenograft (PDX) models of breast cancer (4), and motivates the use of TMT labeling for the analysis of larger cohorts of patients (5).

One substantial shortcoming of quantification by isobaric labeling is the high cost of reagents. We and others have previously reported protocols in which the amount of TMT reagent recommended by the vendor was reduced (6–10) and

From the ‡Chair of Proteomics and Bioanalytics, Technical University of Munich (TUM), Freising, Germany; §Broad Institute of Massachusetts Institute of Technology and Harvard, Cambridge, MA; ¶Max Delbrück Center for Molecular Medicine in the Helmholtz Society, Berlin, Germany; ‖Berlin Institute of Health, Berlin, Germany; **Bavarian Biomolecular Mass Spectrometry Center (BayBioMS), TUM, Freising, Germany

Received February 14, 2019, and in revised form, April 6, 2019
Published, MCP Papers in Press, April 9, 2019, DOI 10.1074/mcp.TIR119.001385

successfully applied such economically optimized labeling workflows to address a variety of biological questions (3, 11–13). However, details on the quantities and concentrations of reactants vary widely in the published literature and, to the best of our knowledge, no systematic evaluation of the influence of reducing TMT-to-peptide ratios on the overall labeling performance has been reported to date.

In the present study, we systematically evaluated the impact of labeling reaction parameters and established a robust and efficient TMT labeling protocol that achieves complete labeling of primary amines in peptides using eight times less TMT reagent than recommended by the vendor. We demonstrate transferability of the protocol between laboratories, provide guidance on the adoption of the optimized approach for different peptide quantities, and show the applicability of the improved protocol to in-depth proteomic and phosphoproteomic analyses.

EXPERIMENTAL PROCEDURES

Experimental Design and Statistical Rationale—The rationale of the experimental design is described in more detail in the respective results sections, and a detailed overview of labeling conditions including quantities, volumes, and concentrations of reactants, buffers, and solvents are listed in the supplement. In three independent experiments, increasing peptide quantities (12.5 to 800 μg) were labeled using the same TMT concentration and quantity (100 or 800 μg) and including, in total, 11 conditions as technical, intralaboratory duplicates or triplicates. Moreover, 17 samples were labeled in three experiments as singlicates, applying different TMT (40 to 400 μg) and peptide (40 or 200 μg) quantities and concentrations to explore the impact of these parameters on labeling performance and to examine the adaptability of optimized protocol parameters to lower peptide quantities. To assess interlaboratory robustness, four labeling experiments, in which the TMT quantity was titrated (50 to 400 μg) against a constant peptide amount (100 μg), were carried out as seven replicates of which two or three were performed in three independent laboratories. All experiments for method optimization were analyzed as single-shot LC-MS/MS runs. To evaluate the utility of the optimized labeling protocol to highly fractionated samples, a deep-scale (phospho)proteome analysis was performed as previously described (4) but using the optimized protocol (*i.e.* using 8x less TMT reagent) and comparing it to the original labeling protocol. Briefly, peptides derived from digests of basal (B) and luminal (L) breast cancer PDX models (WHIM2 and WHIM16) were labeled in five replicates within a TMT10-plex experiment (B-L-B-B-L-B-L-L-B-L) and fractionated using high pH RP chromatography. After pooling and phosphopeptide enrichment, 24 whole proteome and 12 phosphoproteome fractions were measured by LC-MS/MS.

Cell Culture, Lysis, and Protein Digestion—HeLa and Jurkat cells were cultured in DMEM and RPMI 1640 medium, respectively, supplemented with 10% FBS (Gibco™), and 1% antibiotic, antimycotic solution (Sigma). WHIM2 and WHIM16 basal and luminal breast cancer PDX models were generated as previously described (14). Cells, PDX and murine liver tissue were lysed in 8 M urea in 40 mM Tris-HCl, pH 7.6 (Hela), or 75 mM NaCl and 50 mM Tris, pH 8.0 (Jurkat, liver, PDX tissue), containing protease inhibitor and phosphatase inhibitor cocktails. Lysates were incubated on ice for 15 to 30 min followed by centrifugation at 20,000 $\times$ *g* for 10 to 15 min at 4 °C to remove insoluble debris. Protein concentration of the supernatant was determined by the Pierce™ Coomassie or BCA Protein Assay Kit (ThermoScientific). Disulfide bridges were reduced using 10 mM DTT at 30 °C for 30 min (HeLa) or 5 mM DTT at 37 °C for 1 h (Jurkat, mouse liver, PDX tissue). Alkylation was performed at room temperature in the dark using 50 mM chloroacetamide for 30 min (HeLa) or 10 mM iodoacetamide for 45 min (Jurkat, mouse liver, PDX tissue). Lysates were diluted to $<$ 2 M urea using 40 mM Tris-HCl, pH 7.6 (HeLa), or 50 mM Tris-HCl, pH 8.0 (Jurkat, mouse liver, PDX tissue). Digestion was performed by either adding trypsin (Promega) at a 1:50 enzyme-to-substrate ratio and incubating overnight at 37 °C and 600 rpm (HeLa) or by performing a double digestion at 25 °C using 1:50 LysC (Wako) for 2 h and 1:50 trypsin overnight (Jurkat, mouse liver, PDX tissue). Digests were acidified by addition of neat formic acid (FA) to 1%, centrifuged to pellet insoluble matter, and desalted using tC18 RP solid-phase extraction cartridges (Waters Corp.; wash solvent: 0.1% FA or TFA; elution solvent: 0.1% FA in 50% acetonitrile (ACN)). Eluates were frozen at −80 °C and dried by vacuum centrifugation.

TMT Labeling, Peptide Fractionation, and Phosphopeptide Enrichment—Desalted peptides were reconstituted in 0.1% FA and peptide concentration was determined using the Pierce™ BCA Protein Assay Kit. For workflow optimization experiments, the peptide solution was aliquoted accordingly (12.5 to 200 μg peptides), frozen at −80 °C, and dried by vacuum centrifugation. Peptides were reconstituted in 50 mM HEPES (pH 8.5) and TMTzero reagent or a mix of TMT10-plex reagents (ThermoFisher) was added from stocks dissolved in 100% anhydrous ACN. Respective volumes and concentrations are specified in the results section and supplement. The peptide–TMT mixture was incubated for 1 h at 25 °C and 400 rpm, and the labeling reaction was stopped by addition of either 5% hydroxylamine to a final concentration of 0.4% or 8 μl of 1 M Tris, pH 8, and incubation for 15 min at 25 °C and 400 rpm. Peptide solutions were acidified with 45% (v/v) of 10% FA in 10% ACN prior to drying or directly frozen at −80 °C and dried by vacuum centrifugation. For in-depth (phospho)proteome analyses, peptides derived from Lys-C/trypsin digests of luminal and basal PDX tumors were processed as described in Mertins *et al.* (4) but following the optimized TMT labeling protocol. Briefly, 300 μg peptides were dissolved in 60 μl of 50 mM HEPES (pH 8.5), and the labeling reaction was started by addition of 300 μg TMT reagents (15 μl of 56.7 mM (20 μg/μl) TMT stocks in 100% anhydrous ACN). Samples were incubated for 1 h at 25 °C and 1,000 rpm, and the labeling reaction was quenched using 5 μl of 5% hydroxylamine (15 min; 25 °C; 1,000 rpm). Peptide solutions were pooled, frozen at −80 °C, and dried by vacuum centrifugation. Subsequently, TMT-labeled samples were desalted using tC18, RP solid-phase extraction cartridges (Waters Corp.; wash solvent: 0.1% TFA; elution solvent: 0.1% FA in 50% ACN), frozen at −80 °C, and dried by vacuum centrifugation. TMT-labeled peptides were fractionated via high pH RP chromatography using a Zorbax 300 Extend-C18 column (3.5 μm, 4.6 $\times$ 250 mm; Agilent). Peptides were pooled into 24 fractions of which 5% were dried down for whole proteome measurements, and the residual 95% were further pooled into 12 fractions for phosphopeptide enrichment using immobilized metal affinity chromatography. Enrichment was performed using Ni-nitrilotriacetic acid superflow agarose beads (Qiagen) loaded with iron (III) ions. Subsequently, phosphopeptides were desalted using self-packed StageTips (wash solvent: 0.1% FA; elution solvent: 0.1% FA in 50% ACN), frozen at −80 °C, and dried by vacuum centrifugation.

LC-MS/MS Measurements—Tryptic peptides for one-shot analyses were analyzed on an EASY-nLC 1200 or Ultimate 3000 RSLCnano system coupled to a Q-Exactive Plus, Q-Exactive HF-X or

[1] The abbreviations used are: LC, liquid chromatography; MS, mass spectrometry; NCE, normalized collision energy; NHS, N-hydroxysuccinimide; PDX, patient-derived xenograft; PSM, peptide spectrum match; RP, reversed phase; TMT, tandem mass tags.

Fusion Lumos Tribrid mass spectrometer (ThermoFisher Scientific). After reconstitution in 0.1% FA, an amount corresponding to 500 ng peptides was injected. Supplemental Table I provides a detailed overview of LC-MS/MS parameters for the different experiments. In brief, on the Ultimate3000 system, peptides were separated on a 75 μm x 45 cm analytical column (packed in-house with 3-μm C18 resin; Reprosil Gold, Dr. Maisch) applying a flow rate of 300 nl/min and a 20-min linear gradient from 8 to 34% LC solvent B1 (0.1% FA, 5% DMSO in ACN) in LC solvent A1 (0.1% FA in 5% DMSO). The EASY-nLC system was equipped with a 75 μm $\times$ 20 to 22 cm column (Picofrit, New Objective, Inc.; packed in-house with 1.9-μm C18 resin; Reprosil Gold, Dr. Maisch) and operated at a flow rate of 250 or 200 nl/min and applying a 20-min linear gradient from 3 to 55% solvent B2 (90% ACN, 0.1% FA) in A2 (3% ACN, 0.1% FA), a 17-min three-step gradient from 5 to 60% solvent B2 in A2, or a 97-min three-step gradient from 4 to 60% solvent B2 in A2. Mass spectrometers were operated in data-dependent and positive ionization mode. On the Q Exactive Plus, MS1 spectra were recorded at a resolution of 70k using an automatic gain control (AGC) target value of 3e6 or 1e6 charges and maximum injection time (maxIT) of 5 ms or 50 ms. After peptide fragmentation via higher energy collisional dissociation, MS2 spectra of up to 10 precursors were acquired at 17.5k to 70k resolution using an AGC target value of 5e4 and a maxIT of 50 or 120 ms. MS measurements using the Q Exactive HF-X were performed as described above with the following modifications: MS1 spectra were recorded at a resolution of 60k using a maxIT of 10 ms. Fragment spectra were acquired at 30k resolution using a maxIT of 30 ms. The Fusion Lumos was operated as the Q Exactive HF-X with the following modifications: MS1 spectra were acquired using an AGC target value of 4e5 charges. MS2 spectra of up to 20 peptide precursors per cycle were recorded at 15k resolution using a maxIT of 22 ms. Peptides for deep-scale (phospho)proteome analyses were measured as described before (4) using an EASY-nLC coupled to a Fusion Lumos. Briefly, peptides were separated over an 84-min linear gradient from 6 to 30% solvent B2 in A2 at a flow rate of 200 nl/min using a 22-cm column as described above. MS1 spectra were recorded at 60k resolution using an AGC target value of 4e5. MS2 spectra were acquired at 50k resolution using an AGC target value of 6e4 and a maxIT of 105 ms. Cycle time was set to 2 s.

Database Searching—MaxQuant: For peptide and TMT titration experiments, peptide identification and quantification were performed using MaxQuant (version 1.6.3.3) with its built-in search engine, Andromeda (15, 16). Tandem mass spectra were searched against the human reference proteome (UP000005640, 95,936 entries, downloaded on October 12, 2018) and/or the mouse reference proteome (UP000000589, 62,407 entries, downloaded on October 12, 2018) supplemented with common contaminants. Separate searches were conducted to check for under- and overlabeling. For underlabeling evaluation, TMTzero or TMT10 was specified as variable modification on lysine and peptide N termini. For overlabeling assessment, TMTzero or TMT10 was specified as a fixed label on primary amines within a reporter ion MS2 experiment and, additionally, as a variable modification on either histidine or serine, threonine, and tyrosine. For all searches, carbamidomethylated cysteine was set as a fixed modification and oxidation of methionine and N-terminal protein acetylation as variable modifications. Trypsin/P was specified as the proteolytic enzyme with up to two missed cleavage sites allowed. Precursor tolerance was set to $\pm$4.5 ppm, and fragment ion tolerance to $\pm$20 ppm. For modified peptides, default cutoffs of at least 40 and 6 were used for Andromeda score and delta score, respectively. Results were adjusted to 1% false discovery rate on a peptide spectrum match level employing a target–decoy approach using reversed protein sequences.

Database Searching - Spectrum Mill—Raw files of fractionated (phospho)proteomes were searched against the human and mouse RefSeq database containing 37,592 human and 27,289 mouse entries complemented with common contaminants (RefSeq.20160914_Human_Mouse_ucsc_hg19_mm10_customProDBnr_mito_150contams) using Spectrum Mill suite vB.06.01.202 (Broad Institute and Agilent Technologies). Briefly, a four-cycle fixed/mix modifications search strategy that ran four consecutive searches with different sets of modifications in each round and then produced a single integrated output. The four cycles were as follows: all unmodified, both peptide N termini and lysines labeled, only lysines labeled, and only peptide N termini labeled. Carbamidomethylation of cysteines and selenocysteines was set as additional fixed modification. N-terminal protein acetylation, oxidation of methionine, de-amidation of asparagine, hydroxylation of proline (when followed by Gly), and cyclization of peptide N-terminal glutamine and carbamidomethyl cysteine to pyroglutamic acid (pyroGlu) and pyro-carbamidomethyl cysteine, respectively, and TMT overlabeling of serine, threonine, and tyrosine (limited to histidine-containing peptides) were set as variable modifications. For phosphoproteome analysis, phosphorylation of serine, threonine, and tyrosine were allowed as additional variable modifications, while de-amidation of asparagine was restricted to N followed by glycine, and TMT overlabeling and hydroxylation of proline were not allowed. Trypsin Allow P was specified as the proteolytic enzyme with up to four missed cleavage sites allowed. For proteome analysis, the allowed precursor mass shift range was -18 to 262 Da to allow for pyroGlu and up to one additional TMT and two Met-ox per peptide. For phosphoproteome analysis, the range was expanded to -18 to 272 Da to allow for up to three phosphorylations and two Met-ox per peptide. Precursor and product mass tolerances were set to $\pm$20 ppm with PSM-level false discovery rate $<$1% employing a target–decoy approach using reversed protein sequences. To better dissect proteins of human and mouse origin, the subgroup-specific protein grouping option in Spectrum Mill was enabled, details of which were previously described (17).

Bioinformatic Analysis—For estimation of molarities of functional groups in protein digests, an *in silico* digest of the human reference proteome was performed using the Protein Digestion Simulator released by the Pacific Northwest National Laboratory (https://omics.pnl.gov/software/protein-digestion-simulator). To obtain a conservative estimate of primary amines on peptide N termini, cleavage was set to trypsin/P with no missed cleavage sites allowed. Minimum and maximum fragment masses were set to 400 and 6,000 Da, and duplicated sequences for given proteins were included. The average of monoisotopic peptide masses was used to calculate molarities of amino acids in 100 μg digest. For all MS data analyses, hits to the reverse and contaminant databases were removed. For underlabeling analysis, only peptide sequences that were modified with TMT on all lysine side chains and free (*i.e.* not acetylated) peptide N termini were counted as "fully labeled." Peptides that did not bear any TMT were annotated as "not labeled," whereas peptides that contained at least one TMT but were not fully labeled were classified as "partially labeled." N-terminal acetylated arginine peptides were excluded from the underlabeling analyses. Peptides that were identified to be labeled with TMT on at least one serine, threonine, or tyrosine in the overlabeling search were counted as overlabeled. For analysis of fractionated PDX (phospho)proteomes, reporter ion signals were corrected for isotope impurities, and only human and mouse proteins identified with at least two unique peptides were considered for analysis. Relative abundances of proteins and phosphorylation sites were determined using the median of TMT reporter ion intensity ratios from all PSMs matching to the protein or phosphorylation site. PSMs lacking a TMT label, having a precursor ion purity $<$ 50%, or having a negative delta forward–reverse score (half of all false-positive iden-

TABLE I
Theoretical molarity of functional groups in a complete digest of 100 μg of a human proteome. Estimations are based on average peptide length, and pKa values were taken from literature (22, 27)

Functional group	Amount in nmol (100 μg peptides)	pKa
α-amine on N-term	78	7.7 ± 0.5
ε-amine on Lys	38	10.5 ± 1.1
Primary amines	***116***	
Hydroxyl on Tyr	25	10.3 ± 1.2
Hydroxyl on Ser	76	~16
Hydroxyl on Thr	49	~16
Hydroxyl groups	***150***	
Imidazole on His	***24***	6.6 ± 1.0

tifications) were excluded. To normalize quantitative data across TMT10-plex experiments, TMT intensities were divided by the median intensity of all 10 TMT channels for each phosphorylation site and protein. Ratios were further normalized by median centering and median absolute deviation scaling.

RESULTS

Comparative Evaluation of Labeling Efficiency Using the Standard Protocol Versus Reduced Reagent-to-peptide Ratios for High Protein Input—An estimate of the amount of α- and ε-amino groups on peptide N termini and lysine side chains, respectively, yielded ~116 nmol free primary amines in 100 μg peptides derived from an efficiently digested human sample (Table I). The TMT labeling protocol provided by the manufacturer recommends adding 800 μg labeling reagent, which equates to 2.32 μmol of TMT (2.36 μmol in case of TMTzero), to peptides originating from a digest of 25 to 100 μg protein. Hence, the standard protocol uses at least a 20-fold molar excess of the labeling reagent. Even if a certain degree of reagent hydrolysis and overlabeling is taken into account, the TMT reagent is still applied in great excess (Table I). Based on these theoretical considerations, we hypothesized that considerably higher quantities than 100 μg peptides could be labeled using 800 μg TMT reagent. To test this hypothesis, a peptide titration experiment was performed in triplicates using peptide amounts ranging from 100 to 800 μg murine liver peptides, resulting in TMT-to-peptide ratios (wt/wt) of 8:1 up to 1:1. Across labeling reactions, the total reaction volume and thus TMT concentration was kept constant (16.5 mM TMT during labeling), whereas the protein concentration consequently increased with increasing peptide input amounts (Fig. 1*A*). The reaction was stopped by adding Tris, pH 8, to a final concentration of 50 mM.

Single-shot LC-MS/MS analysis led to the identification of between 8,081 and 8,807 peptide sequences with a slight increase with decreasing TMT-to-peptide ratios (Fig. S1*A*). Across the entire range of tested peptide quantities, at least 98.7% of PSMs corresponded to peptides that were fully labeled (Fig. 1*B*). Consequently, few nonlabeled or partially labeled peptides (where either the lysine side chain or peptide N terminus was not labeled) were observed (less than 0.7% of PSMs for all but one outlier sample corresponding to 200 μg peptides). Furthermore, most of the underlabeled PSMs (77–100%) contained at least one TMT modification. The corresponding overlabeling analysis revealed that 10.4 to 14.6% of PSMs contained at least one TMT-labeled serine, threonine, or tyrosine residue, when the labeling reaction was conducted using 100 to 400 μg peptides (Fig. 1*C*). Interestingly, in the 800 μg peptide samples, the fraction of PSMs assigned to overlabeled peptides decreased to less than 3% with only a very small concomitant increase in partially labeled PSMs. For lower peptide quantities, overlabeling primarily affected serine residues (up to 74.2% of overlabeled PSMs), whereas tyrosine residues were overrepresented when using lower TMT-to-peptide ratios (up to 67.3% of overlabeled PSMs; Fig. 1*C*). Of note, 55.5 to 78.1% of overlabeled PSMs contained a histidine residue (Fig. 1*C*). To exclude that this observation was an artifact created by false TMT localization, we re-searched the data, allowing TMT as a variable modification on histidine. Only 1.5% of the spectra were assigned to peptides containing a TMT-labeled histidine and up to 95.7% of these also contained a serine, threonine, or tyrosine residue (data not shown). This indicates that false TMT localization is not a substantial issue. Intensity distributions of overlabeled peptides were comparable to correctly labeled peptides, while underlabeled peptides showed significantly lower intensities (Fig. S1*B*). Taken together, this indicates that the recommended quantity of 800 μg TMT reagent can label at least four to eight times more peptides than what the vendor protocol suggests with a concomitant reduction in overlabeling of undesired amino acid residues.

Downscaling of TMT Quantities Using Optimized Labeling Parameters—Encouraged by the above findings, we subsequently examined whether smaller peptide quantities can be efficiently labeled using less TMT reagent than recommended by the vendor (for an overview of all experiments performed, see Supplemental Table II). From chemical reaction kinetics and the law of mass action, it follows that the efficiency of the labeling reaction depends not only on the absolute quantities of tagging reagent used but, more importantly, on the molar concentrations of the reactants, *i.e.* TMT and peptides or, more precisely, relevant functional groups on peptides. Hence, in order to keep conditions similar to the initial peptide titration experiment, in addition to decreasing TMT and peptide quantities, we also reduced the reaction volume to maintain relatively high concentrations.

Initial experiments were performed using 100 μg TMT reagent and between 12.5 and 200 μg HeLa peptides while decreasing reaction volumes by a factor of 5.6 (Fig. 1*D*). Consequently, labeling took place at TMT concentrations of 11.8 mM, and the reagent-to-peptide ratio varied from 8:1 to 1:2. This time, the reaction was stopped by adding hydroxylamine to a final concentration of 0.4%. Replicate analyses demonstrated that up to 100 μg peptides were efficiently

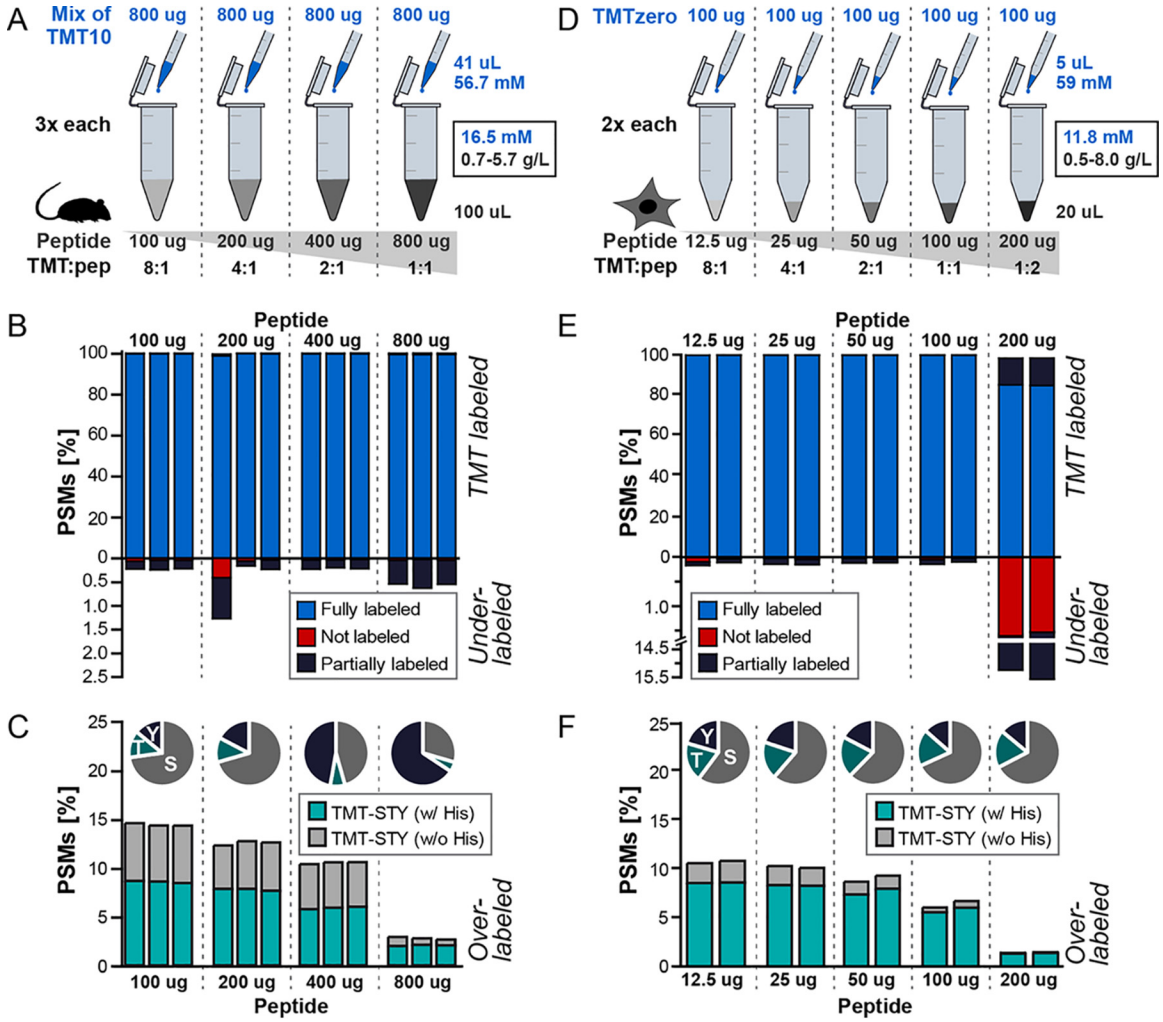

FIG. 1. **Peptide titration experiments using the vendor recommended (*A–C*) and a down-scaled (*D–F*) TMT labeling protocol.** (*A*) Quantities and concentrations of a mix of TMT10-plex reagents (blue) and peptides (gray) are shown for increasing peptide amounts in labeling volumes recommended by the TMT vendor (pep: peptide). The TMT reaction was quenched using 50 mM Tris, pH 8 (final concentration). (*B*) PSMs identifying underlabeled and fully labeled peptides are depicted for intralaboratory replicates using the labeling protocol displayed in (*A*). (*C*) The number of PSMs assigned to overlabeled, O-acylated peptides, and the distribution of serine, threonine, and tyrosine in these spectra are illustrated for the labeling protocol displayed in (*A*). (*D*) Same as (*A*) but using TMTzero and smaller peptide quantities in decreased volumes (pep: peptide). The TMT reaction was quenched using 0.4% hydroxylamine (final concentration). (*D*) Same as (*B*) but for the peptide titration row displayed in (*D*). (*F*) Same as (*C*) but for the peptide titration row depicted in (*D*).

labeled, resulting in 7,005 to 7,906 fully TMT-labeled peptides and a PSM labeling efficiency of 99.8 to 99.9% (single-shot LC-MS/MS analyses; Fig. 1*E*). The lower the TMT-to-peptide ratio was, the higher were the peptide identifications obtained (Fig. S1*C*). For 200 μg peptides (1:2 ratio of TMT-to-peptide), the proportion of PSMs corresponding to partially or nonlabeled peptides sharply increased to an average of 14.9% (Fig. 1*E*), affecting ε-amines of lysine residues more than peptide N termini (18% of all lysine residues *versus* $<$ 4% of all N termini; see Supplemental Table II). The MS1 intensities of underlabeled peptides were again found to be always considerably lower than those of correctly labeled peptides, whereas overlabeled peptides showed comparable intensities (Fig. S1*D*). TMT labeled serine, threonine, and tyrosine residues were present in on average 10.8% of identified spectra for a TMT-to-peptide ratio of 8:1. This fraction decreased to 6.3% and 1.5% for a reagent-to-peptide ratio of 1:1 and 1:2, respectively (Fig. 1*F*). Serine accounted for about two-thirds of the overlabeled amino acids for all peptide quantities used. Again, most of the overlabeled peptides contained a histidine (Fig. 1*F*). In accordance with the first experiment series, a search allowing histidine to be labeled by TMT assigned, on average, 4.6% of the PSMs to peptides with a TMT-labeled histidine residue, and up to 99% of these peptides also comprised at least one serine, threonine, or tyrosine residue (data not shown).

The above findings were corroborated in independent experiments using murine liver tissue. Triplicate experiments

using 100 μg TMT revealed fully labeled peptides in on average 99.7% of PSMs for 100 μg peptides and 42.7% of PSMs for 200 μg peptides (Supplemental Table II). Additional experiments using 200 μg peptides from Jurkat cell and PDX digests showed complete labeling using 200 μg TMT at the same TMT concentration of 11.8 mM (> 99.4% of PSMs identified correctly labeled peptides; see Supplemental Table II). Together, we conclude that, for 100 μg or more peptide quantity, peptides can be efficiently labeled at a TMT-to-peptide ratio of 1:1 and at TMT and peptide concentrations of 11.8 mM and 4 g/l, respectively. We performed another series of labeling experiments using a smaller peptide quantity (40 μg PDX peptides) at TMT-to-peptide ratios ranging from 8:1 to 1:1 and at different TMT (1.4 to 29.5 mM) and peptide concentrations (0.5 to 2.2 g/l; see Supplemental Table II for details). Spectra labeling efficiencies of > 99.6% were obtained in all experiments employing a TMT-to-peptide ratio of at least 2:1. For a TMT-to-peptide ratio of 1:1 at 6.6 mM TMT and 2.2 g/l peptides, 98.2% of PSMs identified fully labeled peptides, but this fraction dropped substantially to 82.1% and 75.7% at lower TMT and peptide concentrations (Supplemental Table II). This illustrates that, for peptide quantities below 100 μg, less than 100 μg TMT can be used if the TMT and peptide concentrations are adapted accordingly.

Assessing Interlaboratory Reproducibility of the Optimized Labeling Protocol—Having established that a TMT-to-peptide ratio of 1:1 (wt/wt) is sufficient to label a proteome efficiently, we sought to show that the results can be reproduced in different laboratories when using identical labeling workflows. To accomplish this, peptides from digests of cryopulverized patient-derived breast cancer xenograft tumors were distributed to our three laboratories, and replicates of 100-μg peptide aliquots were labeled with 50 to 400 μg TMTzero reagent spanning TMT-to-peptide ratios from 4:1 to 1:2 while maintaining a constant reaction volume (Fig. 2*A*). This time, we chose to increase the TMT amount and concentration to be able to assess if doing so would result in differences in over- or underlabeling compared with the previous peptide titration experiments. The labeling reaction was stopped by adding hydroxylamine to a final concentration of 0.4%.

In line with the results above, one-shot LC-MS/MS measurements demonstrated efficient labeling of PDX peptides in all reactions using a TMT-to-peptide ratio of 4:1 to 1:1 (Fig. 2*B*). Despite differences in the overall numbers of identifications between laboratories due to different LC setups and LC/MS instrument performance (3,877 to 7,197 modified peptide sequences, Fig. S2*A*), on average 99.7% of PSMs consistently identified fully labeled peptides. Moreover, the percentage of underlabeling in all experiments was < 0.5% of PSMs (Fig. 2*B*). However, reducing the TMT-to-peptide ratio to 1:2 led to significant underlabeling of between 4.7 and 28.4% of PSMs depending on the laboratory (Fig. 2*B*). Similarly, the fraction of identified spectra assigned to overlabeled peptides differed between laboratories and ranged from 2.6 to 13.3% in efficiently labeled samples (Fig. 2*C*). This fraction dropped by a factor of two to three in experiments using only 50 μg TMT for 100 μg peptides. Again, serine was the predominantly O-acylated amino acid (see Fig. 2*C*), though we observed discrepancies in the fraction of TMT-labeled serine and tyrosine residues among overlabeled peptides in single experiments (see also Figs. 1*C* and 1*F* and Supplemental Table II). Despite evaluating several potential parameters that could influence overlabeling (see discussion), we could not establish a well-founded explanation for these differences. As already observed in the peptide titration experiments, up to 98% of overlabeled peptides also contained a histidine in the sequence (Fig. 2*C*). Consistent with our prior observations, underlabeled peptides exhibited consistently lower MS1 intensities compared with correctly labeled peptides, while overlabeled peptides showed comparable to slightly higher signals (Fig. S2*B*). No apparent difference in the under- or overlabeling trend caused by higher TMT concentrations compared with higher peptide concentrations could be determined when comparing the TMT titration to the peptide titration experiments.

Benchmarking the Optimized Protocol for Deep-scale TMT10-plex (Phospho)proteomic Analyses—After we established in several lines of experiments and across laboratories that a TMT-to-peptide ratio of 1:1 is sufficient to achieve high labeling efficiency judged by single-shot LC-MS/MS analyses, we next evaluated the optimized protocol for deep-scale (phospho)proteome studies. Here, peptides from five replicates of basal and luminal breast cancer PDX models were combined into a TMT10-plex experiment and separated into 24 whole-cell proteome and 12 phosphoproteome fractions. We employed the same workflow as described in Mertins *et al.* (4) but adjusted the TMT labeling step such that only 1/8 of the recommended amount of TMT reagents was used. Specifically, 300 μg of TMT reagent and 300 μg of peptides were labeled per channel in a final volume of 75 μl, and results were benchmarked against the original protocol using 2,400 μg TMT reagents to label 300 μg of peptides in a total volume of 423 μl (Fig. 3*A*). These samples were generated and analyzed in the same laboratory.

Not surprisingly, the observed labeling efficiency was slightly lower for both fractionated TMT10-plex experiments (Fig. 3*B*) compared with the single-shot analysis described above because the fractionation step enabled identification of more of the lower abundant and underlabeled peptides. The overall numbers of collected MS2 spectra, PSMs, distinct (phospho)peptides, and labeling efficiencies were comparable between the two labeling protocols (Fig. 3*B*). Underlabeling at peptide N termini was 2% for the standard protocol and 3% for the reduced TMT protocol, while underlabeling of lysines was 0.5% and 0.6%, respectively. Overlabeling on histidine-containing peptides and fractions of overlabeled serine, threonine, and tyrosine residues were also comparable

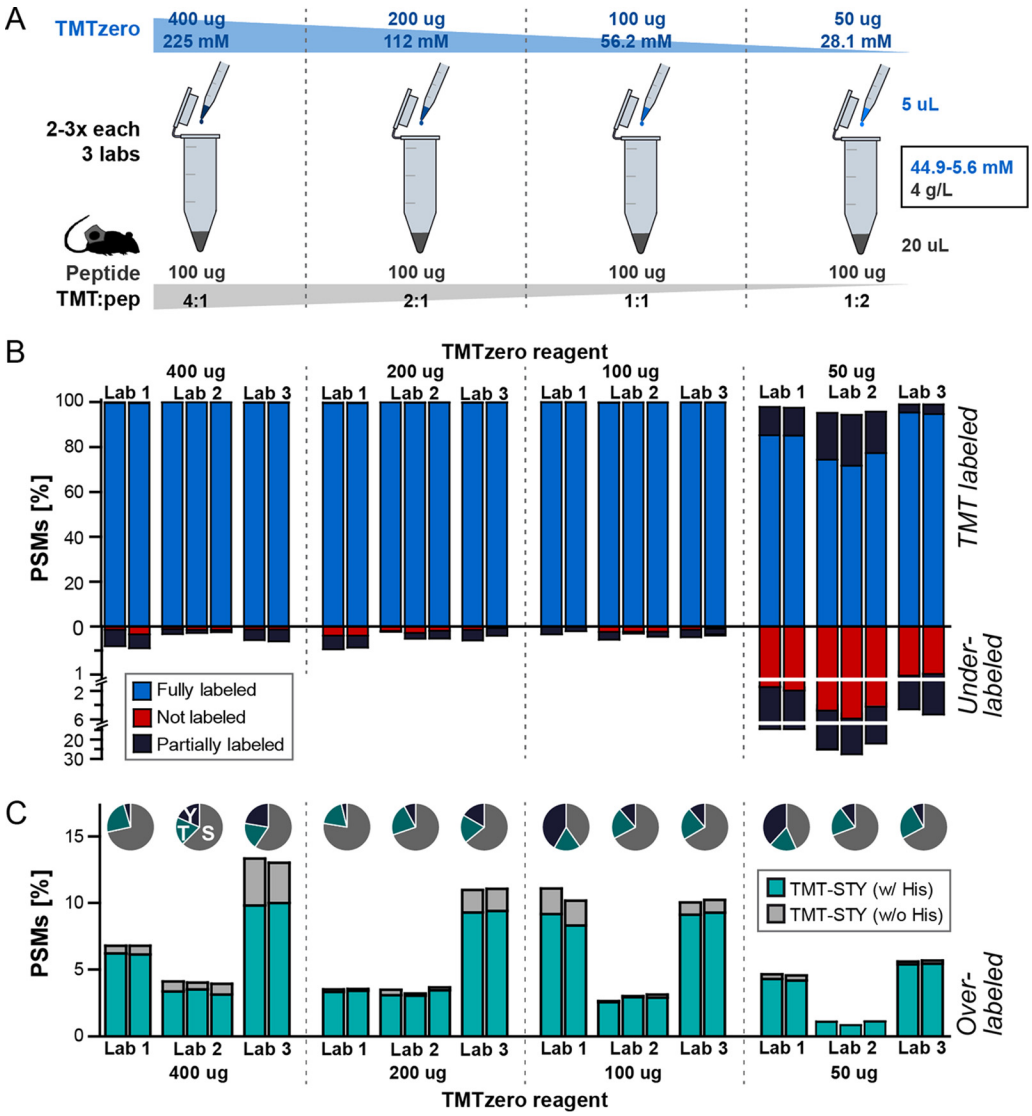

FIG. 2. **TMT titration experiment using the down-scaled TMT labeling strategy across laboratories.** (*A*) Quantities and concentrations of TMTzero reagent (blue) and peptides (gray) are illustrated for increasing TMT quantities in constant labeling volumes (pep: peptide). The TMT reaction was quenched using 0.4% hydroxylamine (final concentration). (*B*) PSMs identifying underlabeled and fully labeled peptides are shown for intra- and interlaboratory replicates following the protocol depicted in (*A*). (*C*) The number of PSMs assigned to overlabeled, O-acylated peptides and the distribution of serine, threonine, and tyrosine in these spectra are displayed for the workflow shown in (*A*).

between the standard (11.4%) and the optimized protocol (11.6% of PSMs, see Fig. S3). More than 12,000 proteins were identified in both experiments, of which > 8,400 were human proteins, and protein identifications showed a large overlap (> 90%) between experiments (Fig. 3*C*). On average, ~42,000 phosphorylation sites were detected (> 35,000 of human origin), and three quarters of these were identified in both workflows (Fig. 3*C*). We observed an excellent intraplex correlation (Pearson > 0.8) of human and murine proteins and phosphopeptides across luminal and basal quintuplicates for both labeling protocols (Fig. 3*D*). Similarly, proteins and phosphopeptides correlated well (Pearson > 0.7) between the two workflows (Fig. 3*D*). Importantly, this interworkflow correlation was comparable to the interplex correlation reported previously for two identical TMT10-plex experiments using the vendor recommended amount of TMT reagent (4). In summary, this demonstrates the utility of the optimized TMT protocol employing 1/8 of the original amount of TMT for deep-scale proteomics and phosphoproteomic studies.

DISCUSSION

The series of labeling experiments shown above using different TMT and peptide concentrations, quantities, and ratios allowed us to systematically assess the influence of these parameters on the labeling reaction. Smaller reaction volumes and, consequently, higher TMT and peptide concentrations were advantageous for labeling efficiency as the law of mass action would demand. Further, the smaller the ratio of TMT to

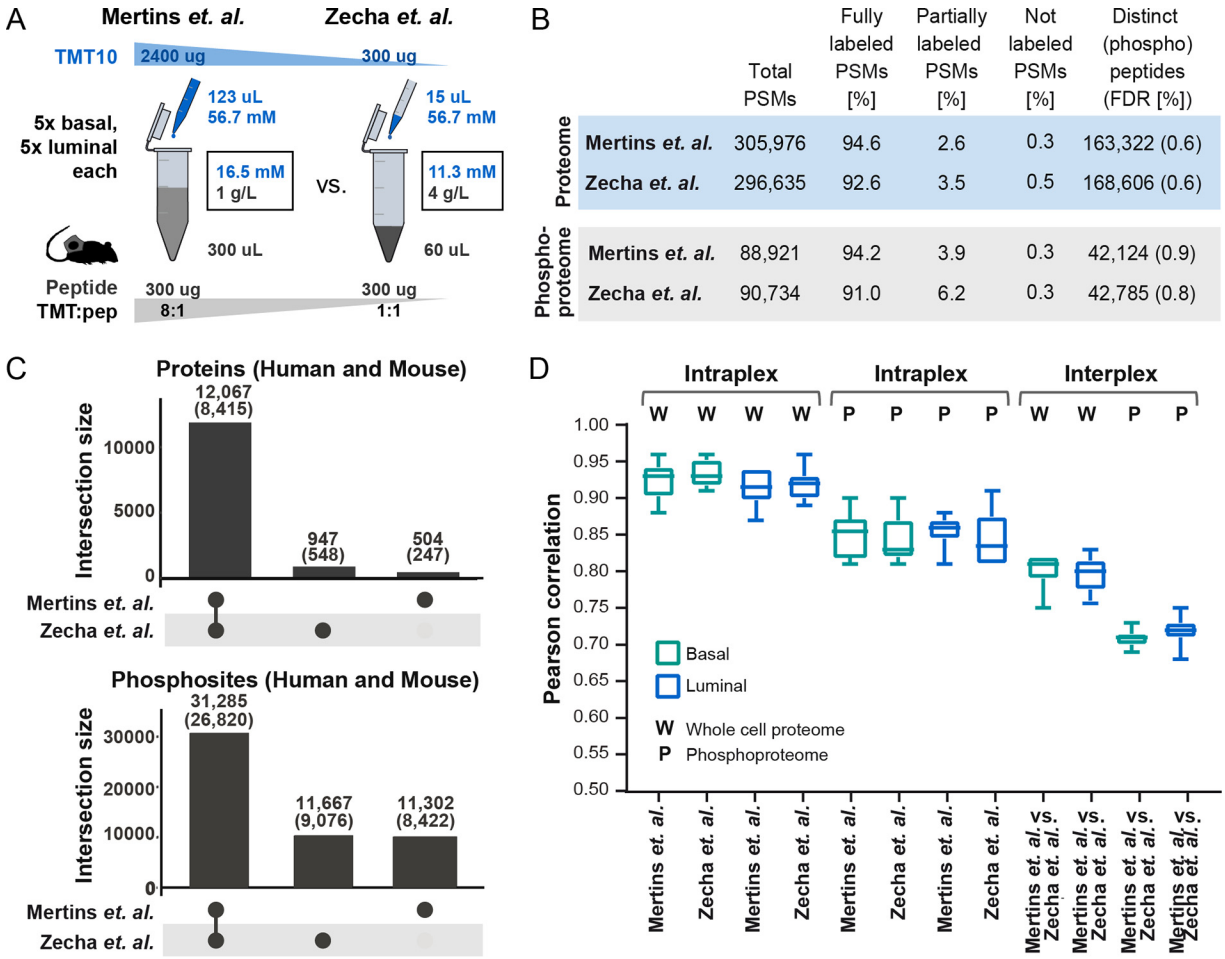

FIG. 3. **Benchmarking the optimized protocol for deep-scale (phospho)proteomic analysis.** (*A*) TMT10-plex experiments were performed using five replicates each of peptides derived from basal and luminal breast cancer PDX models and following the two different labeling protocols displayed here. Quantities and concentrations of TMT10-plex reagents (blue) and peptides (gray) used per channel are shown for the standard (4) and the optimized labeling protocol (3; pep: peptide). (*B*) The table lists the number of total PSMs, PSMs identifying fully and partially labeled peptides, and distinct (phospho)peptides for the whole cell and phosphoproteome analyses following the labeling protocols displayed in (*A*). (*C*) Bar charts illustrate proteins (*upper panel*) and phosphosites (*lower panel*) that were identified for both or only one of the two labeling workflows depicted in (*A*). Proteins and phosphorylation sites mapping to the human database are given in brackets. (*D*) Pearson correlation coefficients are plotted for correlations within TMT10-plex experiments (intraplex) and between TMT10-plex experiments (interplex, *i.e.* inter-workflow) following the protocols depicted in (*A*).

peptides, the more crucial are the concentrations of reagent and peptide. This can be readily explained by the competing reactions of labeling of primary amines and hydrolysis of the TMT reagent in aqueous conditions that contributes to less efficient labeling in less concentrated protein and TMT solutions. Therefore, for reagent-to-peptide ratios of 1:1 (wt/wt), we recommend employing TMT and peptide concentrations of 10 mM (3.4 μg/μl) and 2 g/l, respectively, to ensure efficient labeling. Importantly, peptide concentrations should be determined directly before TMT labeling (as done in this study) because, from experience, 30 to 50% of the initial protein quantity can be lost during digestion and subsequent desalting procedures, and these losses may vary between sample types and laboratories.

Moreover, we stress that careful handling of the TMT reagent is inevitable (as described in the manufacturer protocol) when working with low TMT-to-peptide ratios to avoid loss of active reagent as a result of hydrolysis caused by absorbed water from ambient air. This is of particular relevance when TMT leftovers need to be stored. In our experience, unused TMT reagent can readily be kept in anhydrous ACN at −20 °C or −80 °C for at least 3 months without any drop in labeling efficiencies. For long-term storage, we recommend to aliquot TMT in an inert atmosphere and store it dried down and under exclusion of water. This can easily be realized by performing the aliquoting procedure in a bin filled with argon, and aliquots can be kept under argon or with a desiccant. By this means, we have stored aliquoted TMT reagent for up to a year without any decline in labeling performance.

Although our protocol can, in principle, be adapted to peptide quantities in the low microgram range by appropriately decreasing reaction volumes, handling very small volumes,

particularly TMT reagent in 100% ACN, is not very practical and can lead to inaccuracies. Consequently, we recommend increasing the relative reaction volume for peptide quantities below 50 μg and compensating for the lower TMT and peptide concentrations (*e.g.* 5 mM TMT and 1 g/l peptide) by concomitantly increasing the TMT-to-peptide ratio (*e.g.* to 2:1). For peptide quantities below 10 μg, even higher reagent-to-peptide ratios are likely required (18). Alternatively, it is conceivable that higher ACN concentrations may have a positive effect on labeling efficiency (due to lower reagent hydrolysis) particularly for less concentrated samples or low absolute sample quantities and would facilitate the use of the desired TMT-to-peptide ratio of 1:1. Although this study included labeling experiments at different ACN concentrations, these always also involved variations of other parameters such as TMT or peptide concentration. Hence, a systematic assessment of the influence of ACN on the labeling reaction would require further experiments preferentially using small peptide quantities.

Small changes in the pH of the reaction buffer can also affect labeling efficiency and overlabeling. Typically, more alkaline pH values promote the inactivation of NHS esters due to hydrolysis (19). This is particularly relevant when the excess of the labeling reagent is limited. For example, a TMT-to-peptide ratio of 1:1 roughly corresponds to a 2.5 x molar excess of TMT reagent over the estimated molarity of primary amines in a perfectly digested human proteome. Therefore, the pH (and purity) of the peptide solution must be controlled properly to ensure a reproducible outcome. At the same time, pH values lower than the pK_a values of the primary amines of lysine and peptide N termini result in a higher degree of protonation at equilibrium that hinders the reaction with TMT. Because we performed labeling at pH 8.5, this effect is illustrated by the higher fraction of nonlabeled lysine residues (pK_a $\sim$10.5) compared with N termini (pK_a $\sim$7.7) in all samples that show significant underlabeling in the single-shot analyses. In contrast, we and others have observed the opposite trend of N termini being preferentially underlabeled at pH 8.5 using different TMT, peptide, and ACN concentrations, particularly in samples that show near complete labeling (4, 18). This may be explained by the fact that the higher pK_a value of the ε-amine also typically (depending on the solvent) corresponds to a higher nucleophilicity in the deprotonated state and consequently a higher reactivity toward TMT. Thereby, the labeling of lysine residues may be kinetically favored over peptide N termini under certain conditions. However, which reaction conditions determine preferential underlabeling of either the ε- or α-amine remains elusive and needs further investigation. Notably, it has been shown for pH values of up to 8.5 that the increase in reactivity of both primary amines exceeds the accelerated hydrolysis rate of NHS esters (20, 21), providing the basis for conducting the TMT labeling reaction at pH 8.5.

Considering that the pK_a values of the side chains of lysine and tyrosine are similar (22), one would expect that the reactivity of tyrosine would also increase at elevated pH, rendering it more prone to react with TMT at more basic pH values. However, several studies investigating labeling of amino acids and peptides using NHS esters reported that the abundance of acylated tyrosine residues is enhanced only at a more acidic pH, whereas more alkaline pH values favor N-acylation (20, 21, 23). This may be explained by the lower stability of tyrosine acylation in basic conditions, which can be harnessed to reverse overlabeling by adding hydroxylamine and thus increasing the pH above 9 to quench the labeling reaction (21, 24–26). The reversal of overlabeling by hydroxylamine may also account for the overall lower fraction of O-acylation at higher TMT-to-peptide ratios observed in the titration experiments using 12.5 to 200 μg peptides compared with the ones using 100 to 800 μg peptides. In the latter series of experiments, Tris buffer at pH 8 instead of hydroxylamine was used to quench the labeling reaction.

The high prevalence of TMT-labeled serine and threonine residues may be surprising considering their very high pK_a values (27), which must result in a high degree of protonation of their hydroxyl groups at pH 8.5 and, therefore, a low susceptibility to react with TMT. Indeed, an early study investigating the reactivity of NHS esters toward amino acids could not detect serine and threonine derivatives at pH 7.4 (19). In contrast, others have found before us that hydroxyl-containing amino acids in peptides are reactive toward NHS esters when histidine is in close proximity, notably in -2 or +2 position, to the labeled amino acid (H-X-[STY], [STY]-X-H) (20, 24, 25, 28). This implies that pK_a values can change drastically depending on the molecular environment of amino acids. Indeed, overlabeled peptides were also strongly enriched in histidine in our data, and serine, threonine, or tyrosine residues were 3 to 11 times more likely to be identified in a TMT-labeled state when they were part of the H-X-[STY] motif. The pK_a of histidine is lower than that of N termini (22), which would, in principle, promote histidine modification by TMT. In fact, this has been suggested to occur in solid-phase labeling protocols under slightly acidic conditions (6). However, for our in-solution labeling protocol (performed at basic pH), the results of database searches allowing TMT as a variable modification on histidine provided no plausible evidence that histidine itself is prevalently labeled. This is in accordance with studies reporting a transient, very labile modification of histidine under neutral to alkaline conditions with spontaneous hydrolysis of the formed N-acylimidazole that has a half-life in the range of minutes (19, 23). This may also explain the preferential overlabeling of histidine-containing peptides via an increase in the local concentration of TMT by an initial derivatization of histidine and a subsequent reaction of the N-acylimidazole intermediate with proximal hydroxyl-containing amino acids (20). Besides, histidine could also lead to an increase in the nucleophilicity of hydroxyl-containing amino acids via hydrogen bonding between the side chains resulting in a higher reactivity toward TMT (28). Of

note, the enrichment of histidine in O-acylated peptide sequences likely also accounts for the, on average, higher intensities observed for overlabeled peptides compared with correctly and underlabeled peptides. Irrespective of absolute abundance, histidine-containing peptides exhibit generally higher intensities than non-histidine-containing peptides due to improved ionization mediated by its gas-phase basicity.

Interestingly, we noticed a weak but consistent increase in spectra identification rates with decreasing TMT-to-peptide ratios in all searches of titration experiments specifying TMT as variable modification on lysine and peptide N termini. As already suggested by Böhm *et al.* (6), this increase in identification rates may be ascribed to a reduction in the fraction of overlabeled peptides, which we simultaneously noticed at decreased TMT-to-peptide ratios. A similar observation was made by Miller *et al.,* who detected a higher fraction of modified tyrosine residues with higher reagent-to-peptide ratios (24). This may be a result of different rates of TMT hydrolysis and the reaction with primary amines *versus* hydroxyl groups. O-acylation has been found to proceed up to 20 times slower than N-acylation (23, 24) at least when no histidine was present in close proximity. Therefore, employing relatively low reagent quantities that can be fully consumed by reacting with all primary amines as well as accounting for some reagent hydrolysis would suppress O-acylation and thus reduce overlabeling. Although not investigated here, shortening the reaction time might further minimize overlabeling.

In conclusion, our optimized in-solution labeling procedure reduces the amount of TMT reagent required for efficient labeling of peptides by eightfold relative to the vendor's protocol and thus represents a further improvement of previously published labeling protocols (6–9). The protocol is cost effective without any sacrifice in labeling efficiency or robustness. As demonstrated here, the protocol can easily be adopted and integrated in workflows analyzing cell lines or tissue proteomes. We note that the same principles and parameters investigated in this study may also be applicable to other NHS ester reactions, including iTRAQ labeling, biotinylation, or crosslinking.

Acknowledgments—We thank Guillaume Médard, Susan Klaeger, Sam Myers, and Namrata Udeshi for helpful discussion.

DATA AVAILABILITY

The MS proteomics raw data and complete MaxQuant search results have been deposited to the ProteomeXchange Consortium (http://www.proteomexchange.org/) via the PRIDE (32) partner repository with the data set identifier PXD012703. Spectra identifying modified peptides and proteins on the basis of single peptide matches can be viewed in the MaxQuant Viewer included in the MaxQuant software which has also been deposited in the same location.

* This work was supported in part by grants from the National Cancer Institute (NCI) Clinical Proteomic Tumor Analysis Consortium (grants NIH/NCI U24-CA210986 and NIH/NCI U01 CA214125, and NIH 1U24DK112340 to S.A.C.) and the German Science Foundation (grant SFB1321 to B.K.). B.K. is founder and shareholder of OmicScouts. He has no operational role in the company.

S This article contains supplemental material Supplemental Tables I and II and Figs. S1-S3.

§§ To whom correspondence may be addressed. E-mail: kuster@tum.de.

‡‡ To whom correspondence may be addressed. E-mail: scarr@broad.mit.edu.

Author contributions: J.Z. developed methodology; J.Z., S.S., P.M., S.A.C., and B.K. designed research; J.Z., S.S., T.K., S.A., and M.H.K. performed research; J.Z. and S.S. analyzed data; J.Z. and S.S. prepared figures; and J.Z. wrote the paper with input from S.S., K.C., P.M., S.A.C., and B.K.

REFERENCES

1. Bantscheff, M., Lemeer, S., Savitski, M. M., and Kuster, B. (2012) Quantitative mass spectrometry in proteomics: Critical review update from 2007 to the present. *Anal. Bioanalytical Chem.* **404,** 939–965
2. Thompson, A., Schäfer, J., Kuhn, K., Kienle, S., Schwarz, J., Schmidt, G., Neumann, T., and Hamon, C. (2003) Tandem mass tags: A novel quantification strategy for comparative analysis of complex protein mixtures by MS/MS. *Anal. Chem.* **75,** 1895–1904
3. Zecha, J., Meng, C., Zolg, D. P., Samaras, P., Wilhelm, M., and Kuster, B. (2018) Peptide level turnover measurements enable the study of proteoform dynamics. *Mol. Cell Proteomics* **17,** 974
4. Mertins, P., Tang, L. C., Krug, K., Clark, D. J., Gritsenko, M. A., Chen, L., Clauser, K. R., Clauss, T. R., Shah, P., Gillette, M. A., Petyuk, V. A., Thomas, S. N., Mani, D. R., Mundt, F., Moore, R. J., Hu, Y., Zhao, R., Schnaubelt, M., Keshishian, H., Monroe, M. E., Zhang, Z., Udeshi, N. D., Mani, D., Davies, S. R., Townsend, R. R., Chan, D. W., Smith, R. D., Zhang, H., Liu, T., and Carr, S. A. (2018) Reproducible workflow for multiplexed deep-scale proteome and phosphoproteome analysis of tumor tissues by liquid chromatography–mass spectrometry. *Nat. Protoc.* **13,** 1632–1661
5. Archer, T. C., Ehrenberger, T., Mundt, F., Gold, M. P., Krug, K., Mah, C. K., Mahoney, E. L., Daniel, C. J., LeNail, A., Ramamoorthy, D., Mertins, P., Mani, D. R., Zhang, H., Gillette, M. A., Clauser, K., Noble, M., Tang, L. C., Pierre-François, J., Silterra, J., Jensen, J., Tamayo, P., Korshunov, A., Pfister, S. M., Kool, M., Northcott, P. A., Sears, R. C., Lipton, J. O., Carr, S. A., Mesirov, J. P., Pomeroy, S. L., and Fraenkel, E. (2018) Proteomics, post-translational modifications, and integrative analyses reveal molecular heterogeneity within medulloblastoma subgroups. *Cancer Cell* **34,** 396–410.e398
6. Böhm, G., Prefot, P., Jung, S., Selzer, S., Mitra, V., Britton, D., Kuhn, K., Pike, I., and Thompson, A. H. (2015) Low-pH solid-phase amino labeling of complex peptide digests with TMTs improves peptide identification rates for multiplexed global phosphopeptide analysis. *J. Proteome Res.* **14,** 2500–2510
7. Edwards, A., and Haas, W. (2016) Multiplexed quantitative proteomics for high-throughput comprehensive proteome comparisons of human cell lines. In: Reinders, J., ed. *Proteomics in Systems Biology: Methods and Protocols*, pp. 1–13, Springer New York, New York
8. Ruprecht, B., Zecha, J., Zolg, D. P., and Kuster, B. (2017) High pH reversed-phase micro-columns for simple, sensitive, and efficient fractionation of proteome and (TMT labeled) phosphoproteome digests. In: Comai, L., Katz, J. E., and Mallick, P., eds. *Proteomics: Methods and Protocols*, pp. 83–98, Springer New York, New York
9. Navarrete-Perea, J., Yu, Q., Gygi, S. P., and Paulo, J. A. (2018) Streamlined tandem mass tag (SL-TMT) protocol: An efficient strategy for quantitative (phospho)proteome profiling using tandem mass tag-synchronous precursor selection-MS3. *J. Proteome Res.* **17,** 2226–2236
10. Stepanova, E., Gygi, S. P., and Paulo, J. A. (2018) Filter-based protein digestion (FPD): A detergent-free and scaffold-based strategy for TMT workflows. *J. Proteome Res.* **17,** 1227–1234
11. Koch, H., Wilhelm, M., Ruprecht, B., Beck, S., Frejno, M., Klaeger, S., and Kuster, B. (2016) Phosphoproteome profiling reveals molecular mechanisms of growth-factor-mediated kinase inhibitor resistance in EGFR-overexpressing cancer cells. *J. Proteome Res.* **15,** 4490–4504
12. Paulo, J. A., O'Connell, J. D., Everley, R. A., O'Brien, J., Gygi, M. A., and Gygi, S. P. (2016) Quantitative mass spectrometry-based multiplexing

compares the abundance of 5000 S. cerevisiae proteins across 10 carbon sources. *J. Proteomics* **148,** 85–93
13. Mirzaei, M., Gupta, V. B., Chick, J. M., Greco, T. M., Wu, Y., Chitranshi, N., Wall, R. V., Hone, E., Deng, L., Dheer, Y., Abbasi, M., Rezaeian, M., Braidy, N., You, Y., Salekdeh, G. H., Haynes, P. A., Molloy, M. P., Martins, R., Cristea, I. M., Gygi, S. P., Graham, S. L., and Gupta, V. K. (2017) Age-related neurodegenerative disease associated pathways identified in retinal and vitreous proteome from human glaucoma eyes. *Scientific Reports* **7,** 12685
14. Li, S., Shen, D., Shao, J., Crowder, R., Liu, W., Prat, A., He, X., Liu, S., Hoog, J., Lu, C., Ding, L., Griffith, O. L., Miller, C., Larson, D., Fulton, R. S., Harrison, M., Mooney, T., McMichael, J. F., Luo, J., Tao, Y., Goncalves, R., Schlosberg, C., Hiken, J. F., Saied, L., Sanchez, C., Giuntoli, T., Bumb, C., Cooper, C., Kitchens, R. T., Lin, A., Phommaly, C., Davies, S. R., Zhang, J., Kavuri, M. S., McEachern, D., Dong Yi, Y., Ma, C., Pluard, T., Naughton, M., Bose, R., Suresh, R., McDowell, R., Michel, L., Aft, R., Gillanders, W., DeSchryver, K., Wilson, R. K., Wang, S., Mills, G. B., Gonzalez-Angulo, A., Edwards, J. R., Maher, C., Perou , C. M., Mardis, E. R., and Ellis M. J. (2013) Endocrine-therapy-resistant ESR1 variants revealed by genomic characterization of breast-cancer-derived xenografts. *Cell Rep.* **4,** 1116–1130
15. Cox, J., Neuhauser, N., Michalski, A., Scheltema, R. A., Olsen, J. V., and Mann, M. (2011) Andromeda: A peptide search engine integrated into the MaxQuant environment. *J. Proteome Res.* **10,** 1794–1805
16. Tyanova, S., Temu, T., and Cox, J. (2016) The MaxQuant computational platform for mass spectrometry-based shotgun proteomics. *Nat. Protoc.* **11,** 2301
17. Huang K-l., Li, S., Mertins, P., Cao, S., Gunawardena, H. P., Ruggles, K. V., Mani, D. R., Clauser, K. R., Tanioka, M., Usary, J., Kavuri, S. M., Xie, L., Yoon, C., Qiao, J. W., Wrobel, J., Wyczalkowski, M. A., Erdmann-Gilmore, P., Snider, J. E., Hoog, J., Singh, P., Niu, B., Guo, Z., Sun, S. Q., Sanati, S., Kawaler, E., Wang, X., Scott, A., Ye, K., McLellan, M. D., Wendl, M. C., Malovannaya, A., Held, J. M., Gillette, M. A., Fenyö, D., Kinsinger, C. R., Mesri, M., Rodriguez, H., Davies, S. R., Perou, C. M., Ma, C., Reid Townsend, R., Chen, X., Carr, S. A., Ellis, M. J., and Ding, L. (2017) Proteogenomic integration reveals therapeutic targets in breast cancer xenografts. *Nat. Commun.* **8,** 14864
18. de Graaf, E. L., Pellegrini, D., and McDonnell, L. A. (2016) Set of novel automated quantitative microproteomics protocols for small sample amounts and its application to kidney tissue substructures. *J. Proteome Res.* **15,** 4722–4730
19. Anjaneyulu, P. S. R., and Staros, J. V. (1987) Reactions of N-hydroxysulfosuccinimide active esters. *Int. J. Pept. Protein Res.* **30,** 117–124
20. Mädler, S., Bich, C., Touboul, D., and Zenobi, R. (2009) Chemical cross-linking with NHS esters: A systematic study on amino acid reactivities. *J. Mass Spectrom.* **44,** 694–706
21. Yang, W.-C., Mirzaei, H., Liu, X., and Regnier, F. E. (2006) Enhancement of amino acid detection and quantification by electrospray ionization mass spectrometry. *Anal. Chem.* **78,** 4702–4708
22. Grimsley, G. R., Scholtz, J. M., and Pace, C. N. (2009) A summary of the measured pK values of the ionizable groups in folded proteins. *Protein Sci.* **18,** 247–251
23. Leavell, M. D., Novak, P., Behrens, C. R., Schoeniger, J. S., and Kruppa, G. H. (2004) Strategy for selective chemical cross-linking of tyrosine and lysine residues. *J. Am. Soc. Mass Spectrom.* **15,** 1604–1611
24. Miller, B. T., Collins, T. J., Nagle, G. T., and Kurosky, A. (1992) The occurrence of O-acylation during biotinylation of gonadotropin-releasing hormone and analogs. Evidence for a reactive serine. *J. Biol. Chem.* **267,** 5060–5069
25. Wiktorowicz, J. E., English, R. D., Wu, Z., and Kurosky, A. (2012) Model studies on iTRAQ modification of peptides: Sequence-dependent reaction specificity. *J. Proteome Res.* **11,** 1512–1520
26. Regnier, F. E., and Julka, S. (2006) Primary amine coding as a path to comparative proteomics. *Proteomics* **6,** 3968–3979
27. Englander, S. W., Downer, N. W., and Teitelbaum, H. (1972) Hydrogen exchange. *Annu. Rev. Biochem.* **41,** 903–924
28. Miller, B. T., and Kurosky, A. (1993) Elevated intrinsic reactivity of seryl hydroxyl groups within the linear peptide triads His-Xaa-Ser or Ser-Xaa-His. *Biochem. Biophys. Res. Commun.* **196,** 461–467